

Strong but Reversible Super Fatty Acid Adhesives with Adjustable On–Off Temperature

Chunda Ji, Zekang Lu, Hongxin Zhao, Shuitao Gao, Jianbin Huang, Xinxian Ma,* Bin Zhang,* and Yun Yan*

Cite This: *ACS Appl. Mater. Interfaces* 2025, 17, 17381–17388

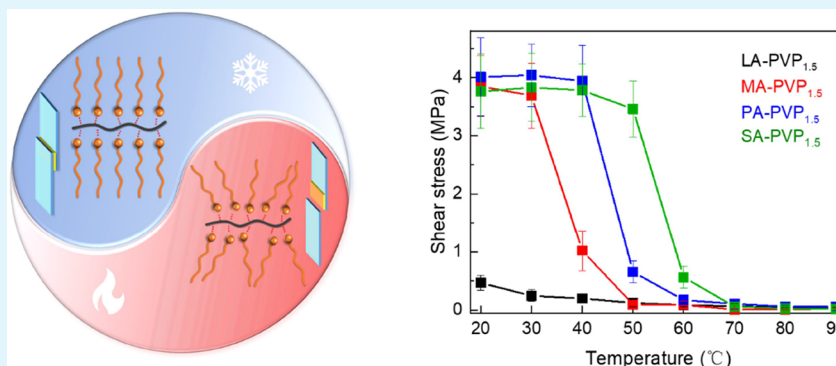
Read Online

ACCESS |

Metrics & More

Article Recommendations

Supporting Information



ABSTRACT: Reversible adhesion is highly desired for intelligent engineering, reassembling devices, and recycling resources. However, many reported reversible adhesives require solvent or pH stimuli to achieve adversity switches, which are very inconvenient for practical applications. So far, thermally responsive adhesives are reported to be very appealing in achieving facile reversible adhesion. However, the fixed on–off switching temperature limits their application in different scenarios. Herein, we report employing fatty acids and polyvinylpyrrolidone to construct supramolecular thermosetting adhesives. The adhesives can switch between solid and liquid states owing to phase transition, resulting in reversible adhesion with a robust strength of ~ 4 MPa and a large on–off ratio of ~ 40 . Upon variation of the chain length of fatty acids, the super fatty acid adhesives can be designed to display reversible adhesion at the desired temperature. This study will open up new inspiration for developing high-performance reversible adhesives for sustainable development.

KEYWORDS: reversible, fatty acid, adhesives, on–off temperature, thermoresponsive

1. INTRODUCTION

Robust yet reversible adhesives are very important in automated production, recycling economics, and sustainable development^{1–4} and are highly desired in fields ranging from electronics,⁵ chips,⁶ medical operations⁷ to transfer printing.⁸ Robust adhesion is highly desired in device fabrication or efficient transferring, whereas excellent deadhesion ability is preferred to achieve repeated operations. Since the former requires unmovable, locked networks,⁹ yet the latter features flowable dynamic chain motion,¹⁰ there exists a great paradox to simultaneously endow a material with high adhesion strength and good reversible attachment, especially those with high on–off adhesion ratios.¹¹

In contrast to the dilemma faced by artificial materials, many creatures in nature have developed elegant biological structures to facilitate reversible adhesion,^{12–15} such as the setae of geckos, the suckers of octopi, and the polygonal arrays of tree frogs. Inspired by these biological strategies, scientists have successfully created quite excellent reversible adhesives that

rely on physical micro/nanostructural engineering,^{1,14,16} but these adhesives usually exhibit very weak adhesion strength below several KPa, which greatly limits their applications.

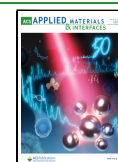
Recently, supramolecular chemistry has displayed promising ability in generating reversible adhesives with enhanced adhesion strength by regulating diversified noncovalent interactions,^{17–20} such as hydrogen bonding,^{21–27} π – π stacking,²⁸ and electrostatic^{29–31} and host–guest interactions.¹⁶ Extraordinary examples can be found in crown-ether-involved polymeric systems that generate switchable adhesion with hydrogen bonding between synthetic monomers and water molecules,^{21,22,32} azobenzene derivative adhesives that

Received: December 20, 2024

Revised: February 25, 2025

Accepted: February 28, 2025

Published: March 10, 2025



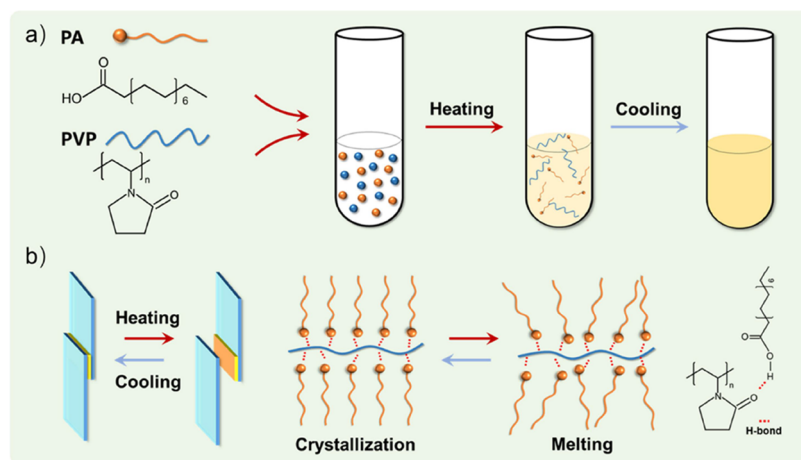


Figure 1. (a) Construction of PA-PVP fatty acid-based reversible adhesives. (b) Molecular mechanism of PA-PVP fatty acid-based reversible adhesives.

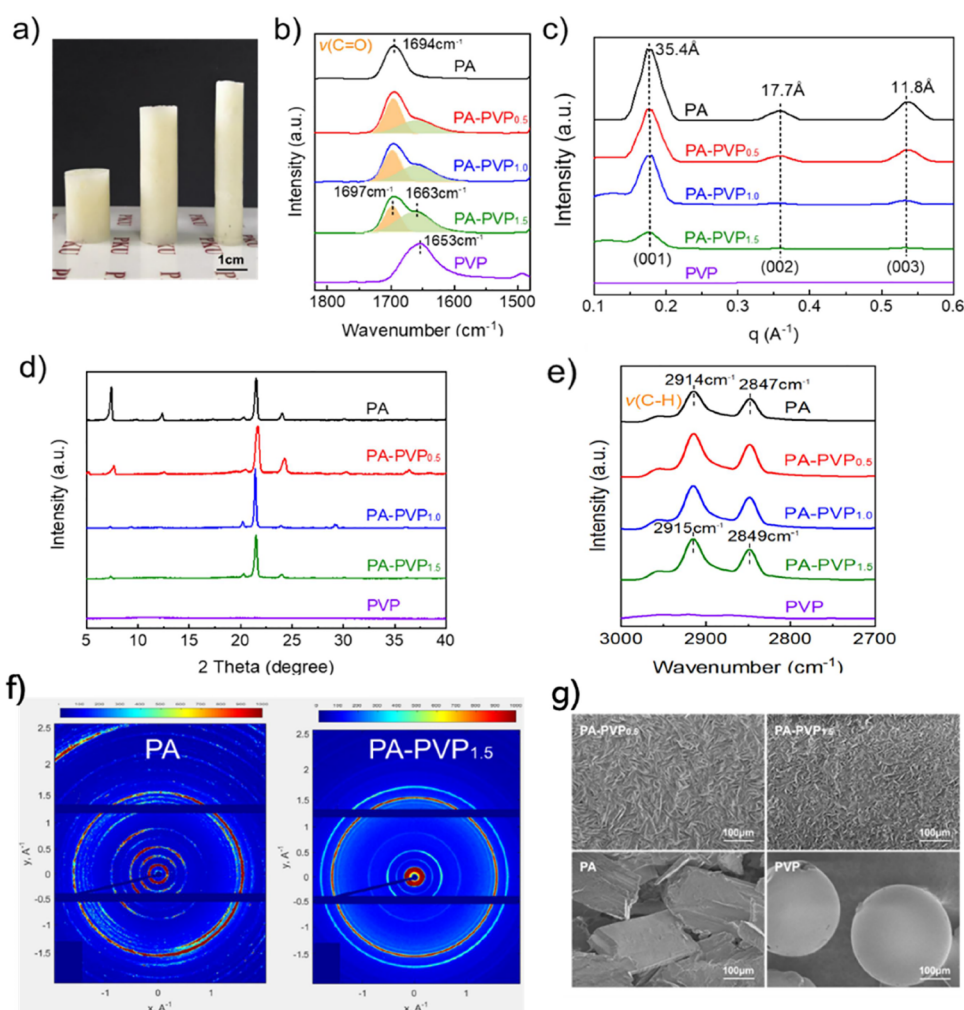


Figure 2. (a) Photograph of PA-PVP_x adhesives. From left to right, $x = 0.5, 1.0, 1.5$, respectively. (b) FT-IR spectra of the C=O stretching vibration for the PA-PVP_x adhesives. (c) One-dimensional WAXS curves, (d) XRD patterns, (e) FT-IR spectra of C-H stretching vibrations, (f) two-dimensional WAXS, and (g) SEM images of PA-PVP adhesives.

regulate π - π interactions through *cis*-*trans* conformation changes,^{28,33} and coordinating supramolecular self-assembly adhesives with temperature-responsive Pt-Pt interactions,³⁴ to name just a few. Albeit the great advances in fundamental science, the above adhesives are still far away from practical

applications due to the complicated chemistry, considerable toxicity, and nonadjustable application conditions.

Fatty acids make up a family of natural substances with long chains. They undergo reversible phase transitions at melting temperature.³⁵⁻³⁷ In particular, the nonfatiguing reversible

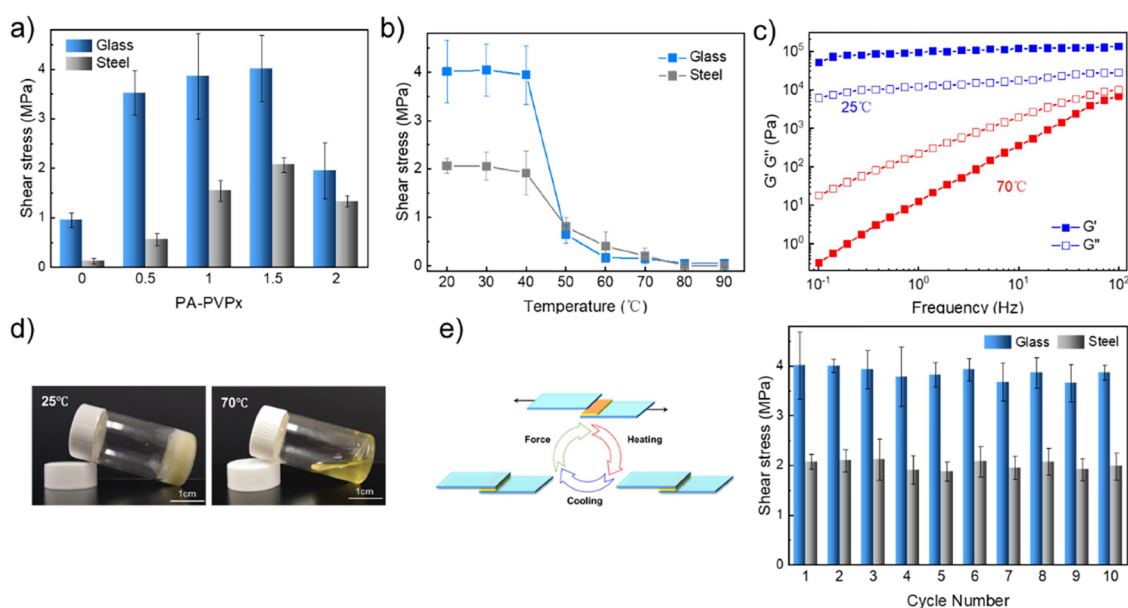


Figure 3. (a) Shear strength of PA-PVP adhesives with different PVP contents. (b) Shear strength of PA-PVP_{1.5} adhesives as a function of temperature. (c) Storage moduli G' and loss moduli G'' of PA-PVP_{1.5} adhesives on frequency sweep at 25 and 70 °C. (d) PA-PVP_{1.5} adhesives' photographs taken at 25 and 70 °C. (e) Shear strength of PA-PVP_{1.5} adhesives after heating-cooling cycles.

liquid–solid phase transition of fatty acids has been widely applied in many fields including batteries,³⁸ building materials,^{39–41} and solar energy storage⁴² for thermal management. In principle, the liquid–solid phase transition of fatty acids can also be utilized in reversible adhesion since the carboxyl groups of fatty acids are able to bind to various surfaces through hydrogen bonding or coordinating interactions, which represent a class of ecofriendly sustainable materials. However, this scenario has not been tested due to the low cohesion force between their hydrocarbon chains.^{43,44} Herein, we report that super fatty acids (SFCs) can be constructed through comelting with a hydrogen-bonding polymer. The resulting SFCs inherit the nonfatiguing reversible liquid–solid phase transition behavior of native fatty acids but with drastically enhanced cohesion force. The maximum shear adhesion strength can be 4 MPa with a large on–off ratio up to 40, which is superior to those of reported reversible adhesives and commonly used commercial glues. Strikingly, the phase transition temperature and shear adhesion strength can be tuned in a wide range to fit different application scenarios by varying the chain length of the fatty acids. We envision that the strategy of SFC would greatly enrich the family of reversible supramolecular adhesives, which is promising for industrial processing, biomedicine, and intelligent transportation.

2. RESULTS AND DISCUSSION

2.1. SFC Preparation and Characterization. The SFCs were prepared by comelting the powder of fatty acids and polyvinylpyrrolidone (PVP). As palmitic acid (PA) was employed, a quantitative mixture of PA-PVP powders was heated to 70 °C, a temperature above the melting point of PA and PVP (Figure S1, Supporting Information), to obtain a homogeneous liquid. After cooling to room temperature, wax-like solids were obtained, as described in Figure 1a. The photographs of the resultant solids are shown in Figure 2a. Here, the adhesives are denoted as PA-PVP_x, where x represents the molar ratio of PVP monomer to PA.

The content of PVP in the PA-PVP_{1.5} adhesive is ~35 wt %, according to TG analysis (Figure S2, Supporting Information). FT-IR measurements in Figure 2b reveal that the C=O stretching vibrations of PVP and PA in PA-PVP_{1.5} occur at 1663 and 1697 cm⁻¹ respectively, which decrease noticeably when compared with PVP (1653 cm⁻¹) and PA (1694 cm⁻¹), indicating the formation of hydrogen bonds between PVP and PA. Meanwhile, Bragg diffractions corresponding to distances of 35.4, 17.7, and 11.8 Å were observed in small-angle X-ray scattering (SAXS, Figure 2c) and X-ray diffraction (Figure 2d) results. These distances feature a spacing ratio of 1:1/2:1/3, corresponding to the (001), (002), and (003) Miller Indices of a lamellar structure, and the lamellae thickness is determined from the (001) diffraction to be 35.4 Å. These lamellae are ascribed to the ordered packing of the alkyl chains of PA, which is reflected by the significantly low C–H symmetric and asymmetric vibration bands around 2547–2549 and 2914–2917 cm⁻¹, respectively (Figure 2e).^{45–48}

Because the extended length of PA is about 21 Å (Figure S3, Supporting Information), the 35.4 Å thickness is much shorter than the two-fold of the PA chain length, indicating that PA molecules have formed staggered bilayers, both on their own and in the coassembly with PVP. It is noteworthy that the bilayer thickness with and without PVP are similar to each other, but FT-IR spectra clearly reveal the formation of hydrogen bonds between PVP and PA, suggesting that PA and PVP have phase-separated at the mesoscale, where small PA crystals are bridged by the PVP chains via hydrogen bonding between them. The significantly reduced PA particle size with increasing PVP content is reflected in the broadened and weakened X-ray scattering or diffraction intensities, as well as the drastically reduced number of concentric rings in the two-dimensional SAXS patterns (Figure 2f). In line with this, SEM observation clearly reveals needle-like granules in the adhesive, which are different from both the PA and PVP single materials. This confirms the formation of PA-PVP coassembled structures, and the size of the coassembled granules decreases with increasing PVP content (Figure 2g).

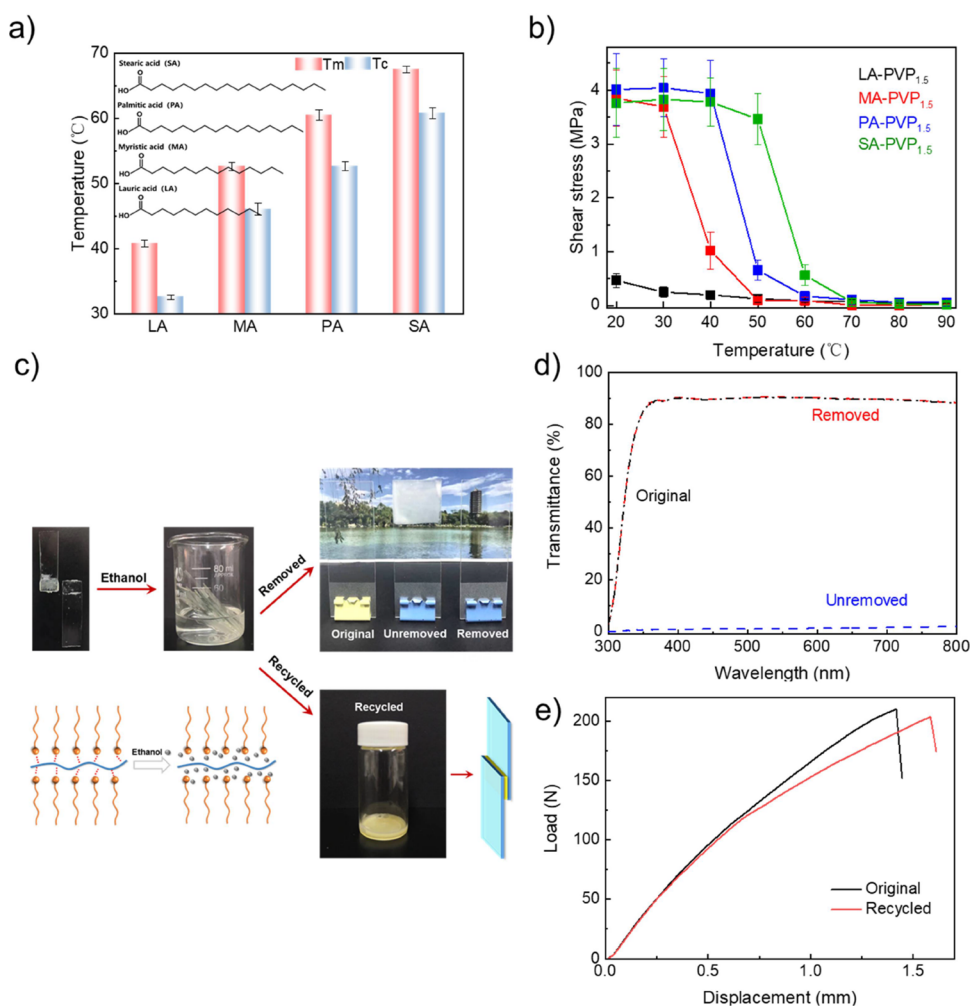


Figure 4. (a) Chemical structures and phase transition point of fatty acids with different chain lengths. (b) Shear strength of fatty acid-based adhesives as a function of temperature. The molar ratio of PVP to fatty acids is constant, at 1.5. (c) Removable and recyclable process of PA-PVP_{1.5} adhesives on glass surfaces. (d) Transmittance of glass before and after adhesive removal. (e) Stress–strain curves of PA-PVP_{1.5} adhesives after recycled.

2.2. Adhesion Properties of PA-PVP_x. Next, the shear adhesion performance of all of the prepared PA-PVP_x adhesives was measured. Upon heating, all of the solids turned into a fluid, which was applied to adhere two pieces of substrates. A mild mechanical pressure of ~ 0.5 MPa was applied during adhesion. After cooling to room temperature, a lap-shear test was performed. Figure 3a shows that the shear strength on glass and steel increases with the PVP content. It is noted that the shear strength reaches a maximum for PA-PVP_{1.5} on both glass and steel, and the value can be up to ~ 4 and ~ 2 MPa, respectively, which is significantly greater than that of pure PA and other commercial adhesives (Figure S4a, Supporting Information). Clearly, PVP has efficiently enhanced the internal cohesion strength of the PA-PVP adhesive through hydrogen bonding between PVP and PA, as shown in Figure 2b, which brings about high adhesion strength. Excessive PVP would reduce the adhesion strength, which is probably due to the further decrease in the size of the PA crystalline granules. The larger PA granules may act as hard cores between the PVP chains, which is advantageous for high internal cohesion force in adhesives. This high internal cohesion also enables strong adhesion of PA-PVP_{1.5} to other substrates, including wood and different materials and plastics

(Figure S4b, Supporting Information). It is noted that the adhesive displays similar adhesion strength on wood as on glass, but very weak adhesion to nonpolar plastics, such as PE and PTFE, which confirms that the surface adhesion is attributed to the formation of hydrogen or coordination bonds between the adhesive and the substrates. Interlocks between rough surfaces are also beneficial for strong adhesion. As a result, the too smooth surface of steel displays much weaker adhesion than copper, and the rough surface of wood exhibits very strong adhesion.

As expected, the PA-PVP adhesives are reversible. The adhesion performance of PA-PVP_{1.5} on glass at different temperatures was measured, and the results are shown in Figure 3b. A sharp decrease of shear strength was observed at temperatures beyond 40 °C, which is attributed to the phase transition of PA in the PA-PVP_{1.5} adhesive (Figure S5, Supporting Information). DSC measurements revealed that above 40 °C, the PA-PVP_{1.5} adhesives begin to melt, which causes a drastic decrease in adhesion strength. Figure 3b shows that the shear strength is reduced to ~ 0.1 MPa at 70 °C. Compared with the initial strong adhesion of ~ 4 MPa, the on–off ratio is as large as ~ 40 . Rheological measurements in Figure 3c reveal that the storage modulus (G') of PA-PVP_{1.5} is

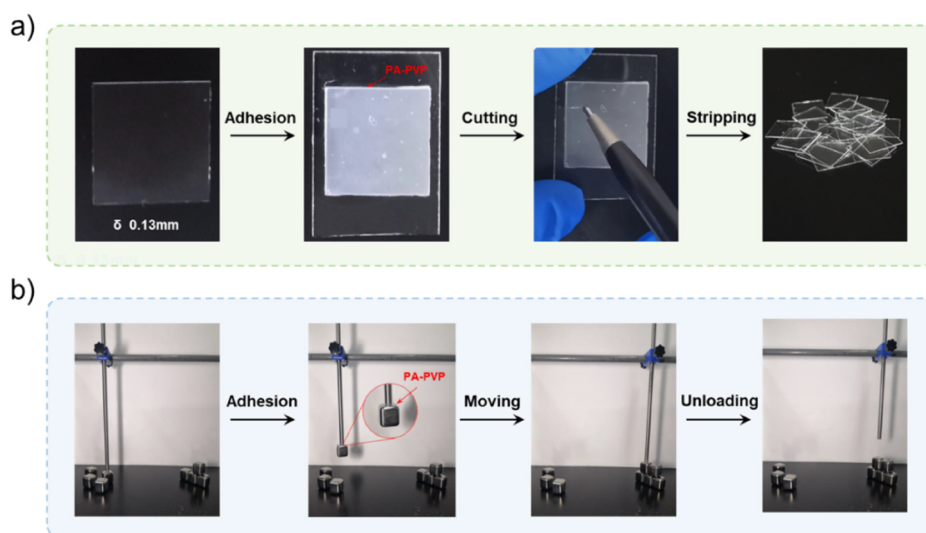


Figure 5. Application diagram of PA-PVP adhesives. (a) Ultrathin material cutting. (b) Intelligent transportation.

lower than its loss modulus (G'') at 70 °C, characteristics of a liquid. In contrast, the storage modulus (G') is up to 10^5 MPa, which is ~ 10 times higher than the loss modulus (G'') at 25 °C and remains nearly constant in the measured frequency range, typical performance for solids. Figure 3d clearly demonstrates the solid–liquid phase states of the PA-PVP_{1.5} adhesive at different temperatures. Because the phase transition is a physical change, which is reversible without changes in covalent bonds, PA-PVP_{1.5} displays excellent reversible adhesion ability. Figure 3e shows that the shear strength of PA-PVP_{1.5} remains unchanged in cycled heating–cooling tests for glass and steel. Similar reversible heating–cooling cycles are observed for PA-PVP_{1.5} on other substrates (Figure S4b of the Supporting Information).

2.3. Temperature Adjustable, Removable, and Recyclable Abilities. The phase transition temperature is relevant to practical applications. By change of the chain lengths of fatty acids, the phase transition temperature of the adhesives can be manipulated to meet application requirements (Figure 4a). Figure 4b shows that the adhesion on–off switching temperature increases with increasing fatty acid chain lengths, which is in accordance with their increasing phase transition temperature (Figure S6, Supporting Information). The shear adhesion strength decreases significantly at 50 °C for the SA-PVP adhesives, while it decreases at 30 °C for MA-PVP adhesives (below room temperature for LA-PVP). This wide range of threshold on–off adhesion temperatures indicates that fatty acid-based adhesives are adaptable to multiscenario applications of reversible adhesion simply by adjusting their chain lengths.

Removability is another criterion for reversible adhesives since clean surfaces are desired in practical applications, such as chip cutting and transferring. Figure 4c shows that the PA-PVP_{1.5} adhesives can be readily removed by soaking in ethanol, which destroys the hydrogen bonding between PA and PVP. After removal of the adhesive, the transmittance of the glass is the same as the original, while it is $\sim 0\%$ for the unremoved (Figure 4d). FT-IR measurements confirm that there is no adhesive residue on the glass surface (Figure S7 in the Supporting Information). Moreover, the removed adhesive can also be recycled by evaporation of ethanol, and the adhesion

strength of the recycled adhesive remains the same as the original (Figure 4e).

2.4. Application of PA-PVP. Chip cutting of ultrathin materials is essential in modern high technology, yet it is very difficult to achieve because the cutting blade often causes inevitable breaking of the ultrathin materials. However, with the help of reversible PA-PVP adhesives, the ultrathin materials can be well-supported and protected by a proper substrate to avoid breaking. Figure 5a demonstrates a case of the perfect cutting of a thin cover glass that is 0.13 mm thick. Before cutting, the cover glass was fixed onto a thick glass plate with the PA-PVP adhesive, and the cutting was conducted on the thick glass plates. After heating the thick glass plate with the adhered cutting cover glass to 70 °C, the small pieces of cover glass were peeled off. Following this, by cleaning with ethanol, the final glass chips are obtained with high yield and quality. This reversible adhesion can also be applied in “intelligent transportation”, as described in Figure 5b. The goods can be adhered to the mobile arm upon cooling of the hot adhesive, which can be unloaded at desired places upon heating.

3. CONCLUSIONS

Reversible saturated fatty acid adhesives are constructed from fatty acids and PVP through hydrogen bonding. The hydrogen bond formation between fatty acids and PVP yields supramolecular solids with retained ordered packing of the fatty acid chains, thus allowing the supramolecular solids to display phase transition behavior just like the fatty acids on their own. With the hydrogen bonds' enhanced internal cohesion force in the solids, the adhesive can achieve a high shear adhesion strength of ~ 4 MPa. Owing to the reversible phase transition of fatty acids, the exemplified PA-PVP_{1.5} adhesives show excellent reversible adhesion with a large on–off ratio of ~ 40 , and the adhesion strength remains unchanged after heating–cooling cycling. Manipulation of the phase transition temperature of super fatty acid adhesives can be achieved by changing the chain length of the fatty acids. We envision that super fatty acid adhesives are promising materials for multiscenario applications ranging from industrial processing and biomedicine to intelligent transportation and fine device engineering.

4. EXPERIMENTAL SECTION

4.1. Materials. Polyvinylpyrrolidone (PVP, M_w 30,000) was purchased from Sigma-Aldrich Corporation. Palmitic acid (PA, >98%) and other fatty acids were obtained from Aladdin Reagent Ltd. All reagents were of AR grade.

4.2. Preparation. Reversible adhesives, PA-PVP, were constructed from PA and PVP by heating and cooling. PA and PVP were mixed in a determined ratio in a flask and heated at 70 °C for 10 min, then cooled to room temperature. Finally, a light-yellow solid was obtained, which is the PA-PVP adhesive. Here, the adhesives were denoted as PA-PVP _{x} , where x represents the molar ratio of the PVP monomer to PA.

4.3. Characterization and Measurements. Scanning electron microscopy (SEM, Hitachi S-4800) was employed to observe the morphology of the PA-PVP adhesives at an acceleration voltage of 1 kV. Two-dimensional (2D) wide-angle X-ray scattering (WAXS) of PA-PVP adhesives was obtained by using a Ganesha system (SAXSLAB, US) equipped with a multilayer focused Cu K α radiation as the X-ray source (Genix 3D Cu ULD) and a semiconductor with LaB $_6$ for the wide-angle region and silver behenate for the small-angle region. X-ray diffraction (XRD) measurements were taken by using a Rigaku Dmax-2400 diffractometer with Cu K α radiation. The phase transition of PA-PVP was measured by a differential scanning calorimeter (DSC, Q2000) at a heating/cooling rate of 10 °C/min. The lap-shear adhesion experiments were performed using a WDW3020 electronic universal testing machine with a 2000 N load cell. The specimens, with a rectangular shape, were used for adhesion experiments at a loading rate of 100 mm/min, and the shear adhesion strength was obtained by dividing the force by the coating area of the PA-PVP adhesives. For shear strength tests at different temperatures, the adhered samples were kept in an oven for 2 h for equilibrium before testing. Each test was performed within 1 min, assuming that the temperature of the sample remains unchanged.

■ ASSOCIATED CONTENT

Data Availability Statement

The data that support the findings of this study are available from the corresponding author upon reasonable request.

Supporting Information

The Supporting Information is available free of charge at <https://pubs.acs.org/doi/10.1021/acsami.4c22030>.

DSC curves for PA, PVA and all the fatty acid-PVA adhesives; TG, FT-IR results and POM images for PA-PVA adhesives; Chem3D modeling of PA molecules; comparison of shear strengths of commercial adhesives vs PA-PVP_{1,5} adhesive; and shear strengths of PA-PVP_{1,5} adhesive after heating-cooling cycles on different substrates (PDF)

■ AUTHOR INFORMATION

Corresponding Authors

Xinxian Ma – Ningxia Key Laboratory of Green Catalytic Materials and Technology, College of Chemistry and Chemical Engineering, Ningxia Normal University, Guyuan 756000, P.R. China; orcid.org/0000-0001-6977-1346; Email: maxinxian@163.com

Bin Zhang – Beijing National Laboratory for Molecular Sciences (BNLMS), State Key Laboratory for Structural Chemistry of Unstable and Stable Species, College of Chemistry and Molecular Engineering, Peking University, Beijing 100871, P.R. China; Email: binzhang@pku.edu.cn

Yun Yan – Ningxia Key Laboratory of Green Catalytic Materials and Technology, College of Chemistry and Chemical Engineering, Ningxia Normal University, Guyuan 756000, P.R. China; Beijing National Laboratory for

Molecular Sciences (BNLMS), State Key Laboratory for Structural Chemistry of Unstable and Stable Species, College of Chemistry and Molecular Engineering, Peking University, Beijing 100871, P.R. China; orcid.org/0000-0001-8759-3918; Email: yunyan@pku.edu.cn

Authors

Chunda Ji – Ningxia Key Laboratory of Green Catalytic Materials and Technology, College of Chemistry and Chemical Engineering, Ningxia Normal University, Guyuan 756000, P.R. China; Beijing National Laboratory for Molecular Sciences (BNLMS), State Key Laboratory for Structural Chemistry of Unstable and Stable Species, College of Chemistry and Molecular Engineering, Peking University, Beijing 100871, P.R. China

Zekang Lu – Beijing National Laboratory for Molecular Sciences (BNLMS), State Key Laboratory for Structural Chemistry of Unstable and Stable Species, College of Chemistry and Molecular Engineering, Peking University, Beijing 100871, P.R. China

Hongxin Zhao – Beijing National Laboratory for Molecular Sciences (BNLMS), State Key Laboratory for Structural Chemistry of Unstable and Stable Species, College of Chemistry and Molecular Engineering, Peking University, Beijing 100871, P.R. China

Shuitao Gao – Beijing National Laboratory for Molecular Sciences (BNLMS), State Key Laboratory for Structural Chemistry of Unstable and Stable Species, College of Chemistry and Molecular Engineering, Peking University, Beijing 100871, P.R. China

Jianbin Huang – Beijing National Laboratory for Molecular Sciences (BNLMS), State Key Laboratory for Structural Chemistry of Unstable and Stable Species, College of Chemistry and Molecular Engineering, Peking University, Beijing 100871, P.R. China

Complete contact information is available at:

<https://pubs.acs.org/doi/10.1021/acsami.4c22030>

Notes

The authors declare no competing financial interest.

■ ACKNOWLEDGMENTS

This work was supported by the National Natural Science Foundation of China (NSFC 22332001, 22202006).

■ REFERENCES

- (1) Lee, H.; Lee, B. P.; Messersmith, P. B. A reversible wet/dry Adhesive Inspired by Mussels and Geckos. *Nature* **2007**, *448* (7151), 338–341.
- (2) Baik, S.; Kim, D. W.; Park, Y.; Lee, T.-J.; Ho Bhang, S.; Pang, C. A wet-Tolerant Adhesive Patch Inspired by Protuberances in Suction Cups of Octopi. *Nature* **2017**, *546* (7658), 396–400.
- (3) Ye, Z.; Lum, G. Z.; Song, S.; Rich, S.; Sitti, M. Phase Change of Gallium Enables Highly Reversible and Switchable Adhesion. *Adv. Mater.* **2016**, *28* (25), 5088–5092.
- (4) Tan, D.; Wang, X.; Liu, Q.; Shi, K.; Yang, B.; Liu, S.; Wu, Z. S.; Xue, L. Switchable Adhesion of Micropillar Adhesive on Rough Surfaces. *Small* **2019**, *15* (50), No. 1904248.
- (5) Zhuo, S.; Zhao, Z.; Xie, Z.; Hao, Y.; Xu, Y.; Zhao, T.; Li, H.; Knubben, E. M.; Wen, L.; Jiang, L.; Liu, M. Complex Multiphase Organohydrogels with Programmable Mechanics Toward Adaptive Soft-Matter Machines. *Sci. Adv.* **2020**, *6*, No. eaax146.
- (6) Yi, H.; Hwang, I.; Sung, M.; Lee, D.; Kim, J.-H.; Kang, S. M.; Bae, W.-G.; Jeong, H. E. Bio-inspired adhesive systems for Next-

Generation Green Manufacturing. *International Journal of Precision Engineering and Manufacturing-Green Technology* **2014**, *1* (4), 347–351.

(7) Li, J.; Celiz, A. D.; Yang, J.; Yang, Q.; Wamala, I.; Whyte, W.; Seo, B. R.; Vasilyev, N. V.; Suo, Z.; Mooney, D. J. Tough Adhesives for Diverse Wet Surfaces. *Science* **2017**, *357*, 378–381.

(8) Kim, S.; Wu, J.; Carlson, A.; Jin, S. H.; Kovalsky, A.; Glass, P.; Liu, Z.; Ahmed, N.; Elgan, S. L.; Chen, W.; Ferreira, P. M.; Sitti, M.; Huang, Y.; Rogers, J. A. Microstructured Elastomeric Surfaces with Reversible Adhesion and Examples of Their Use in Deterministic Assembly by Transfer Printing. *Proc. Natl. Acad. Sci. U. S. A.* **2010**, *107* (40), 17095–17100.

(9) Román, J. K.; Wilker, J. J. Cooking Chemistry Transforms Proteins into High-Strength Adhesives. *J. Am. Chem. Soc.* **2019**, *141* (3), 1359–1365.

(10) Heinzmann, C.; Weder, C.; de Espinosa, L. M. Supramolecular Polymer Adhesives: Advanced Materials Inspired by Nature. *Chem. Soc. Rev.* **2016**, *45* (2), 342–358.

(11) Raos, G.; Zappone, B. Polymer Adhesion: Seeking New Solutions for an Old Problem. *Macromolecules* **2021**, *54* (23), 10617–10644.

(12) Chen, Y.; Meng, J.; Gu, Z.; Wan, X.; Jiang, L.; Wang, S. Bioinspired Multiscale Wet Adhesive Surfaces: Structures and Controlled Adhesion. *Adv. Funct. Mater.* **2019**, *30* (5), No. 1905287.

(13) Bartlett, M. D.; Croll, A. B.; King, D. R.; Paret, B. M.; Irschick, D. J.; Crosby, A. J. Looking Beyond Fibrillar Features to Scale Gecko-Like Adhesion. *Adv. Mater.* **2012**, *24* (8), 1078–1083.

(14) Hofman, A. H.; van Hees, I. A.; Yang, J.; Kamperman, M. Bioinspired Underwater Adhesives by Using the Supramolecular Toolbox. *Adv. Mater.* **2018**, *30* (19), No. 1704640.

(15) Cho, H.; Wu, G.; Christopher Jolly, J.; Fortoul, N.; He, Z.; Gao, Y.; Jagota, A.; Yang, S. Intrinsically Reversible Superglues via Shape Adaptation Inspired by Snail Epiphragm. *Proc. Natl. Acad. Sci. U. S. A.* **2019**, *116* (28), 13774–13779.

(16) Zhao, Y.; Wu, Y.; Wang, L.; Zhang, M.; Chen, X.; Liu, M.; Fan, J.; Liu, J.; Zhou, F.; Wang, Z. Bio-inspired Reversible Underwater Adhesive. *Nat. Commun.* **2017**, *8* (1), 2218.

(17) Zhang, Q.; Shi, C. Y.; Qu, D. H.; Long, Y. T.; Feringa, B. L.; Tian, H. Exploring a Naturally Tailored Small Molecule for Stretchable, Self-healing, and Adhesive Supramolecular Polymers. *Sci. Adv.* **2018**, *4*, No. eaat8192.

(18) Faghhihnejad, A.; Feldman, K. E.; Yu, J.; Tirrell, M. V.; Israelachvili, J. N.; Hawker, C. J.; Kramer, E. J.; Zeng, H. Adhesion and Surface Interactions of a Self-Healing Polymer with Multiple Hydrogen-Bonding Groups. *Adv. Funct. Mater.* **2014**, *24* (16), 2322–2333.

(19) Heinzmann, C.; Coulibaly, S.; Roulin, A.; Fiore, G. L.; Weder, C. Light-Induced Bonding and Debonding with Supramolecular Adhesives. *ACS Appl. Mater. Interfaces* **2014**, *6* (7), 4713–4719.

(20) Sun, P.; Li, Y.; Qin, B.; Xu, J.-F.; Zhang, X. Super Strong and Multi-Reusable Supramolecular Epoxy Hot Melt Adhesives. *ACS Materials Letters* **2021**, *3* (7), 1003–1009.

(21) Dong, S.; Leng, J.; Feng, Y.; Liu, M.; Stackhouse, C. J.; Schönhals, A.; Chiappisi, L.; Gao, L.; Chen, W.; Shang, J.; Jin, L.; Qi, Z.; Schalley, C. A. Structural water as an essential comonomer in supramolecular polymerization. *Sci. Adv.* **2017**, *3*, No. eaao0900.

(22) Li, X.; Lai, J.; Deng, Y.; Song, J.; Zhao, G.; Dong, S. Supramolecular Adhesion at Extremely Low Temperatures: A Combined Experimental and Theoretical Investigation. *J. Am. Chem. Soc.* **2020**, *142* (51), 21522–21529.

(23) Kim, K.; Shin, M.; Koh, M.-Y.; Ryu, J. H.; Lee, M. S.; Hong, S.; Lee, H. TAPE: A Medical Adhesive Inspired by a Ubiquitous Compound in Plants. *Adv. Funct. Mater.* **2015**, *25* (16), 2402–2410.

(24) Wang, S.; Liu, Z.; Zhang, L.; Guo, Y.; Song, J.; Lou, J.; Guan, Q.; He, C.; You, Z. Strong, Detachable, and Self-healing Dynamic Crosslinked Hotmelt Polyurethane Adhesive. *Materials Chemistry Frontiers* **2019**, *3* (9), 1833–1839.

(25) Beharaj, A.; McCaslin, E. Z.; Blessing, W. A.; Grinstaff, M. W. Sustainable polycarbonate adhesives for dry and aqueous conditions with thermoresponsive properties. *Nat. Commun.* **2019**, *10*, 5478.

(26) Feldstein, M. M.; Bovaldinova, K. A.; Bermesheva, E. V.; Moscalets, A. P.; Dormidontova, E. E.; Grinberg, V. Y.; Khokhlov, A. R. Thermo-Switchable Pressure-Sensitive Adhesives Based on Poly(vinyl caprolactam) Non-Covalently Cross-Linked by Poly(ethylene glycol). *Macromolecules* **2014**, *47* (16), 5759–5767.

(27) Hwang, J.; Lim, D.; Lee, G.; Kim, Y. E.; Park, J.; Baek, M. J.; Kim, H. S.; Park, K.; Ku, K. H.; Lee, D. W. Ambient air-operated thermo-switchable adhesion of isopropylacrylamide-incorporated pressure sensitive adhesives. *Mater. Horiz.* **2023**, *10* (6), 2013.

(28) Wu, Z.; Ji, C.; Zhao, X.; Han, Y.; Müllen, K.; Pan, K.; Yin, M. Green-Light-Triggered Phase Transition of Azobenzene Derivatives toward Reversible Adhesives. *J. Am. Chem. Soc.* **2019**, *141* (18), 7385–7390.

(29) Zhang, J.; Chen, Z.; Zhang, Y.; Dong, S.; Chen, Y.; Zhang, S. Poly(ionic liquid)s Containing Alkoxy Chains and Bis(trifluoromethanesulfonyl)imide Anions as Highly Adhesive Materials. *Adv. Mater.* **2021**, *33* (30), No. 2100962.

(30) Gao, S.; Qi, J.; Jiang, S.; Wu, T.; Wang, W.; Cai, Y.; Ma, C.; Zhang, B.; Huang, J.; Yan, Y. Green Wood Adhesives from One-Pot Coacervation of Folic Acid and Branched Poly(ethylene imine). *ACS Appl. Bio Mater.* **2021**, *4* (9), 7314–7321.

(31) Gao, S.; Wang, W.; Wu, T.; Jiang, S.; Qi, J.; Zhu, Z.; Zhang, B.; Huang, J.; Yan, Y. Folic Acid-Based Coacervate Leading to a Double-Sided Tape for Adhesion of Diverse Wet and Dry Substrates. *ACS Appl. Mater. Interfaces* **2021**, *13* (29), 34843–34850.

(32) Liu, L.; Liu, Z.; Ren, Y.; Zou, X.; Peng, W.; Li, W.; Wu, Y.; Zheng, S.; Wang, X.; Yan, F. A Superstrong and Reversible Ionic Crystal-Based Adhesive Inspired by Ice Adhesion. *Angew. Chem., Int. Ed.* **2021**, *60* (16), 8948–8959.

(33) Zhou, Y.; Chen, M.; Ban, Q.; Zhang, Z.; Shuang, S.; Koynov, K.; Butt, H.-J.; Kong, J.; Wu, S. Light-Switchable Polymer Adhesive Based on Photoinduced Reversible Solid-to-Liquid Transitions. *ACS Macro Lett.* **2019**, *8* (8), 968–972.

(34) Wang, Z.; Huang, K.; Wan, X.; Liu, M.; Chen, Y.; Shi, X.; Wang, S. High-Strength Plus Reversible Supramolecular Adhesives Achieved by Regulating Intermolecular Pt II ...Pt II Interactions. *Angew. Chem., Int. Ed.* **2022**, *61* (40), No. e202211495.

(35) Zhang, R.; Chen, D.; Chen, L.; Cao, X.; Li, X.; Qu, Y. Preparation and Thermal properties Analysis of Fatty Acids/1-hexadecanol Binary Eutectic Phase Change Materials Reinforced with TiO₂ Particles. *Journal of Energy Storage* **2022**, *51*, No. 104546.

(36) Akhiani, A. R.; Mehrali, M.; Tahan Latibari, S.; Mehrali, M.; Mahlia, T. M. I.; Sadeghinezhad, E.; Metselaar, H. S. C. One-Step Preparation of Form-Stable Phase Change Material through Self-Assembly of Fatty Acid and Graphene. *J. Phys. Chem. C* **2015**, *119* (40), 22787–22796.

(37) Liu, C.; Li, F.; Ma, L.-P.; Cheng, H.-M. Advanced Materials for Energy Storage. *Adv. Mater.* **2010**, *22* (8), E28–E62.

(38) Huang, Q.; Li, X.; Zhang, G.; Wang, Y.; Deng, J.; Wang, C.; Chen, T. Pouch Lithium Battery with a Passive Thermal Management System Using Form-Stable and Flexible Composite Phase Change Materials. *ACS Applied Energy Materials* **2021**, *4* (2), 1978–1992.

(39) Sipponen, M. H.; Henn, A.; Penttilä, P.; Österberg, M. Lignin-fatty Acid Hybrid Nanocapsules for Scalable Thermal Energy Storage in Phase-Change Materials. *Chemical Engineering Journal* **2020**, *393*, No. 124711.

(40) Ao, C.; Yan, S.; Zhao, S.; Hu, W.; Zhao, L.; Wu, Y. Stearic Acid/Expanded Graphite Composite Phase Change Material with High Thermal Conductivity for Thermal Energy Storage. *Energy Reports* **2022**, *8*, 4834–4843.

(41) Fan, Z.; Zhao, Y.; Ding, Y.; Shi, Y.; Liu, X.; Jiang, D. Fabrication and Comprehensive Analysis of Expanded Perlite Impregnated with Myristic Acid-based Phase Change Materials as Composite Materials for Building Thermal Management. *Journal of Energy Storage* **2022**, *55*, No. 105710.

(42) Aydın, A. A. Fatty Acid Ester-based Commercial Products as Potential New Phase Change Materials (PCMs) for Thermal Energy Storage. *Sol. Energy Mater. Sol. Cells* **2013**, *108*, 98–104.

(43) Liu, H.; Geng, H.; Zhang, X.; Wang, X.; Hao, J.; Cui, J. Hot Melt Super Glue: Multi-Recyclable Polyphenol-Based Supramolecular Adhesives. *Macromol. Rapid Commun.* **2022**, *43* (7), No. 2100830.

(44) Deng, Y.; Zhang, Q.; Feringa, B. L.; Tian, H.; Qu, D. H. Toughening a Self-Healable Supramolecular Polymer by Ionic Cluster-Enhanced Iron-Carboxylate Complexes. *Angew. Chem., Int. Ed.* **2020**, *59* (13), 5278–5283.

(45) Yan, Y.; Xiong, W.; Huang, J. B.; Li, Z. C.; Li, X. S.; Li, N. N.; Fu, H. L. Organized Assemblies in Bolaamphiphile/Oppositely Charged Conventional Surfactant Mixed Systems. *J. Phys. Chem. B* **2005**, *109* (1), 357–364.

(46) Dou, X. Y.; Gao, S. T.; Lu, Z. K.; Huang, J. B.; Yan, Y. Effect of the Molecular Weight of Polyelectrolyte and Surfactant Chain Length on the Solid-Phase Molecular Self-Assembly. *J. Phys. Chem. B* **2023**, *127* (50), 10923–10930.

(47) Qi, J. W.; Wu, T. Y.; Wang, W. K.; Jin, H. J.; Gao, S. T.; Jiang, S. S.; Huang, J. B.; Yan, Y. Solid-phase Molecular Self-assembly Facilitated Supramolecular Films with Alternative Hydrophobic/Hydrophilic Domains for Skin Moisture Detection. *Aggregate* **2022**, *3* (2), No. e173.

(48) Yan, Y.; Huang, J. B.; Li, Z. C.; Ma, J. M.; Fu, H. L.; Ye, J. P. Vesicles with Superior Stability at High Temperature. *J. Phys. Chem. B* **2003**, *107* (7), 1479–1482.